Proceedings of the 13th Annual IEEE International
Conference on Nano/Micro Engineered and Molecular Systems
April 22-26, 2018, Singapore

Fabrication of Low-cost Microfluidic Chip for Terahertz Detection Applications

Salman Alfihed[1,2*], M. H. Bergen[1], Jonathan F. Holzman[1], and Ian G. Foulds[1]
[1] School of Engineering, University of British Columbia (UBC), Kelowna, Canada
[2] Materials Science Research Institute, King Abdulaziz City for Science and Technology (KACST), Riyadh, Saudi Arabia
*E-mail: salfihed@alumni.ubc.ca

***Abstract*-Terahertz time-domain spectroscopy (THz-TDS) is an effective method for materials detection and identification at the macro scale, however, integration of microfluidic chips with THz spectroscopy is still needed to miniaturize this detection technology. Taking into consideration the polymer and micro-fabrication cost, several factors play an important role in the integration of such a technology, the optical absorption of the chip material is one of the significant factors. In this work, we study THz absorption spectra of two low-cost polymers as potential THz microfluidic chip materials, polyethylene terephthalate (PET) and ultra-high-molecular-weight polyethylene (UHMWPE). We then micro-fabricated two identical chips, one made by using PET and the other chip using UHMWPE to measure the absorption spectrum of Sylgard®184 silicone elastomer curing-agent (PDMS-CA) as a low-absorption test fluid.**

Keywords: THz-TDS; lab-on-a-chip; low-cost microfluidics; THz absorption coefficient

I. INTRODUCTION

The use of terahertz (THz) spectroscopy is growing due to the range of detection and sensing applications that THz enables [1]. The wavelengths located between 100-1000 μm, which are equivalent to 0.3-3 THz frequencies, are used in THz applications [2]. The THz frequencies are generated by a photoconductive dipole antenna, which has the capability to generate and detect a THz pulse [3]. The demonstration of subpicosecond photoconducting dipole antennas was the starting point for the emergence of THz-time-domain spectroscopy (THz-TDS) [4]. The technique of THz-TDS has proven to be a powerful measurement tool for characterizing materials in the THz spectrum [5]. Furthermore, THz-TDS is a non-destructive measurement method, and due to its low photon energy, there is a low possibility of tissue damage in biological and medical applications [4]. Figure 1 shows a schematic diagram of a THz-TDS system.

The integration of microfluidic chips with THz optoelectronics is promising for improving measurement processes and miniaturizing analysis systems [6]. The microfluidic chip material is a key factor for microfluidic chip integration with the THz-TDS system. Historically, microfluidics fabrication was based on glass and silicon. However, these materials can be difficult to work with and can require advanced equipment for fabrication. Thus, there has been move toward Poly-(dimethylsiloxane) (PDMS). It offers optical transparency in the visible range and ease of fabrication [7]. The cost of polymers, along with their optical transparency and chemical stability are attractive aspects for the polymer-based microfluidics devices in comparison with silicone-based or glass-based microfluidics devices [8]. While PDMS is one of the lower-cost commonly used materials for microfluidic chip fabrication [9], it does not present a flat absorption spectrum in the targeted range from 0.35 to 1.0 THz [10]. Conversely, cyclic olefin copolymer (COC) has one of the lowest THz absorption spectra in the range 0.5-2.5 THz [11], but it is not a low-cost polymer.

In this work, we study THz absorption versus frequency of two low-cost polymers, polyethylene terephthalate (PET) and ultra-high-molecular-weight polyethylene (UHMWPE). The detection accuracy of the fabricated chips is tested using Sylgard®184 silicone elastomer curing-agent (PDMS-CA) as a low-absorption fluid in the microfluidic channel. The THz-TDS measurements in the range 0.35-1.0 THz are used to extract values for refractive indices and absorption coefficients.

II. MATERIALS AND METHODS

The THz pulse is generated by a 775-nm ultrafast pulsed laser (Toptica Photonics FFS-SYS-2B) with a pulse duration of 100 fs and repetition rate of 90 MHz. The femtosecond laser pulses are split into a pump beam, focused on the THz photoconductive dipole antenna, and a probe beam, which passes through a controlled delay line and is directed by a pellicle beamsplitter through polarization-sensitive optics onto a photodetector. The THz measurement takes place in a nitrogen-filled environment to minimize the effect of water-vapour absorption on the spectroscopic results. The setup is shown in Fig. 1. The detected time-domain waveforms consisting of the THz electric field are Fourier-transformed to reveal the frequency-domain responses. A reference measurement is subtracted from the sample measurement to provide the phase distributions as a function of frequency, *f*. The frequency-dependent refractive index is determined based upon the phase distribution. The absorption coefficient as a function of frequency, *f*, is calculated based upon the estimated refractive index. In this investigation, the two bulk polymers were measured using a collimated THz beam, while the fluid was measured using a focused THz beam.

978-1-5386-5273-2/18/$31.00 © 2018 IEEE

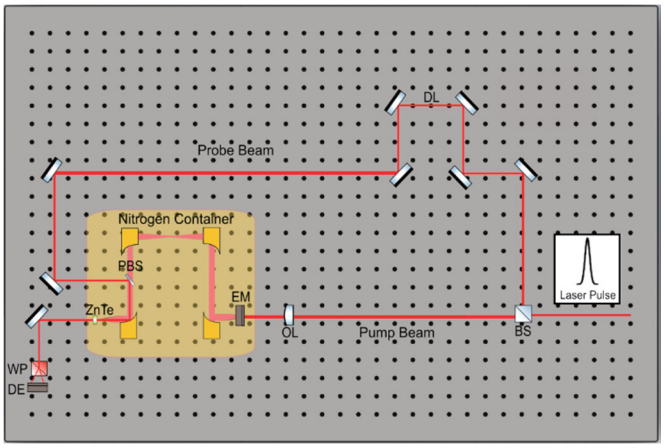

Fig. 1 Schematic diagram of THz-TDS system. Femtosecond laser pulses is split by the beamsplitter (BS) into two beams: one is the pump beam, which is focused by objective lens (OL) to the THz emitter (EM), and the other is the probe beam, which is delayed by the delay line (DL), split by the pellicle beamsplitter (PBS) and passed through polarization-sensitive optics (WP). The THz-TDS measurements take place in a Nitrogen (N_2) container to minimize water vapour absorption.

In the absorption investigation of the two polymers, the PET layers were thermally bonded at 110°C for 60 minutes to form a 0.65-mm-thick PET sample. A 25.6-mm-thick UHMWPE sample was produced by thermal bonding of UHMWPE layers at 145°C for 120 minutes. The two polymer samples were used to determine their THz absorption coefficient in the investigated THz range. However, varying thicknesses were studied initially to determine the optimum thickness of each polymer, based upon their respective absorption coefficients. Generally, high absorption materials need thinner samples to accurately measure the absorption coefficient. The optimum thickness of a measured material d_{opt} depends upon the absorption coefficient, as a function of frequency $\alpha(f)$, and can be obtained by [12]

$$d_{\text{opt}} = \frac{2}{\alpha(f)} \quad (1)$$

After studying the THz absorption of the two polymers, two 76-µm-thick layers of PET (or UHMWPE) were used as THz windows that sandwiched the tested fluid. A CO_2 laser (full spectrum laser – H-Series 20x12) was used to cut 50.8-mm-diameter circles of 2.4-mm-thick sheets of poly (methyl methacrylate) (PMMA) at a laser power of 30 W. Then, an inlet hole with a 1 mm diameter was made on one of the PET (or UHMWPE) layers using a micro-milling machine (Proxxon 37110 Micro Mill MF 70). The two PET layers were then thermally bonded at 105°C for 30 minutes onto the PMMA to create a THz window on the chip. In the case of UHMWPE, a solvent (Methylene diphenyl diisocyanate) was used to bond two UHMWPE layers onto the PMMA to fabricate the chip as shown in Fig. 2.

The PDMS-CA was used to test the UHMWPE chips detection accuracy by way of THz-TDS with a focused beam. Since the fluid has an absorption coefficient below 11 cm^{-1} in

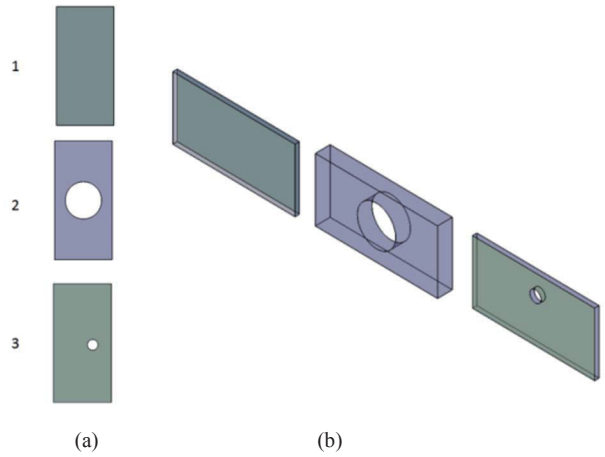

Fig. 2 a) Top view and b) side view of the microfluidic chip that is used to study PDMS-CA. It has multiple elements: 1) bottom layer of PET (or UHMWPE) with a 76 µm thickness, 2) PMMA platform with a 2.4 mm thickness, including a 50.8-mm-diameter THz scanning window, and 3) top layer of PET (or UHMWPE) with a 76 µm thickness, including a liquid inlet.

the targeted range, the optimum chip thickness is in the range of 2-4 mm, based on equation (1). Thus, the thickness of the fabricated chip was chosen to be 2.4 mm. Internal reflections within the fabricated chip are neglected due to the chosen chip thickness, which has a large cavity roundtrip time and a correspondingly small free spectral range in the frequency spectrum. Thus, internal reflections have minimal influence on the THz spectra.

The absorption coefficient of the PDMS-CA is obtained in the two-fabricated chips from 0.35 to 1.0 THz, and compared to study the direct effect of the chip material on the absorption coefficient of the tested material. The refractive index of the low-absorption chip material was compared with the PDMS-CA refractive index to study the reflection path through the fabricated chip.

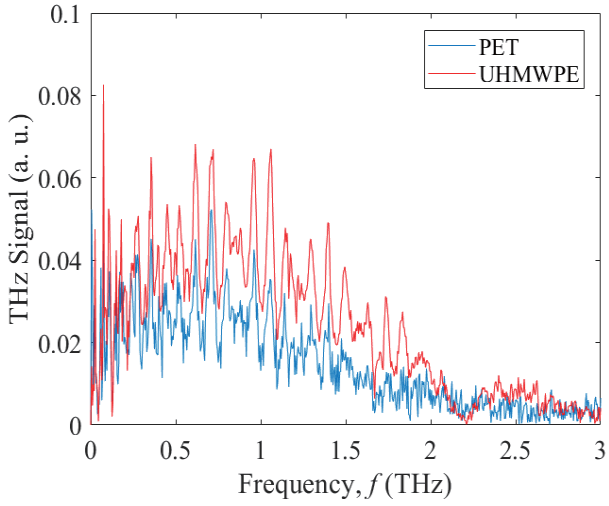

Fig. 3 The THz signal of 0.65-mm-thick PET (blue curve) and 25.6-mm-thick UHMWPE (red curve) in the frequency range from 0 – 3 THz. The figure shows that the UHMEPE sample has higher THz signal levels than the PET sample. The two signals rapidly decrease after 1.5 THz based upon the utilized THz-TDS system.

III. Results and Discussion

Figure 3 shows the Fourier-transformed THz signal of 0.65-mm-thick PET (blue curve) and 25.6-mm-thick UHMWPE (red curve) as a function of frequency, *f*, from 0 to 3 THz. The figure shows that the THz signal of UHMWPE is higher than the PET signal. This is due to the higher absorption of PET in comparison to UHMWPE, even though the UHMWPE sample is nearly 40 times thicker than the PET sample. The signal-to-noise ratio (SNR) decreases steadily with frequency. Both signals decay substantially after 1.5 THz. In the upcoming investigations, we focus on the frequency range from 0.35 THz to 1.0 THz, which has the best signal strength in the utilized THz-TDS system.

Figure 4 shows the THz absorption coefficient of PET (blue curve) and UHMWPE (red curve) as a function of frequency, *f*. It shows the much lower absorption of UHMWPE in comparison with PET. The absorption coefficient of PET rapidly increases from 3.3 cm^{-1} at 0.35 THz to 8.9 cm^{-1} at 1.0 THz. In contrast, the absorption coefficient of UHMWPE shows values below 0.2 cm^{-1} within the targeted range.

The comparison of the refractive indices of UHMWPE and PDMS-CA is shown in Fig. 5. The refractive index of UHMWPE is roughly constant at 1.53, while the refractive index of the PDMS-CA varies within the range of 1.51 to 1.57. This variation, in comparison with PDMS-CA's refractive index, provides minimal changes in loss due to the reflection, while taking into consideration the 76-µm-thick layer of the chip windows.

Figure 6 shows the results of PDMS-CA detection in the PET chip (red curve) and UHMWPE chip (blue curve). Such results are collected to demonstrate the polymer's potential as a low-cost and low-absorption material for the THz spectrum. The figure shows the absorption spectrum of PDMS-CA in the UHMWPE chip without contributions from absorption by the microfluidic chip material.

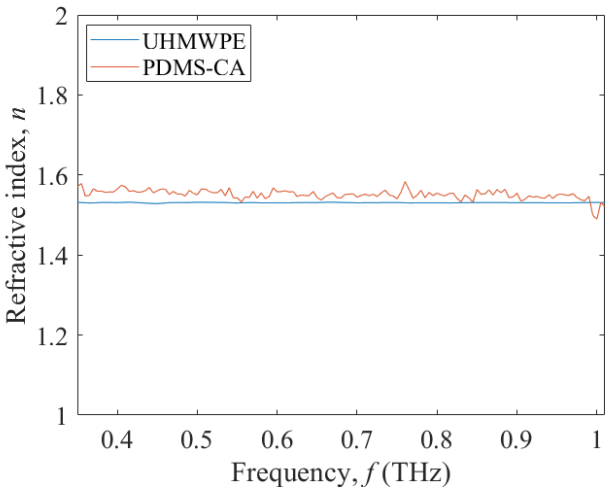

Fig. 5 The refractive indices of the UHMWPE (blue curve) and PDMS-CA (red curve) in the range of 0.35 to 1.0 THz. The measured refractive index of UHMWPE is roughly 1.53, and the measured refractive index of the PDMS-CA is within the range of 1.51 to 1.57.

The selected chip thickness is optimal for low absorption fluids, according to the chip-thickness estimation from equation 1, for the targeted spectral range. In contrast, the absorption coefficient spectrum of PDMS-CA in the PET chip is higher in the range between 0.35-1.0 THz, due to the contributions of the chip material (PET) on the spectrum. For the UHMWPE chip, the absorption coefficient increased from 2.62 cm^{-1} at 0.35 THz to 9.75 cm^{-1} at 1.0 THz. For the PET chip, the absorption coefficient increased from 3.42 cm^{-1} at 0.35 THz to 11.24 cm^{-1} at 0.83 THz, then it is decreased to 10.98 cm^{-1} at 1.0 THz. As a general trend of the two spectrums, the PDMS-CA in the PET chip shows higher absorption over 0.35 to 1.0 THz in comparison to the UHMWPE chip. This behaviour will be discussed next.

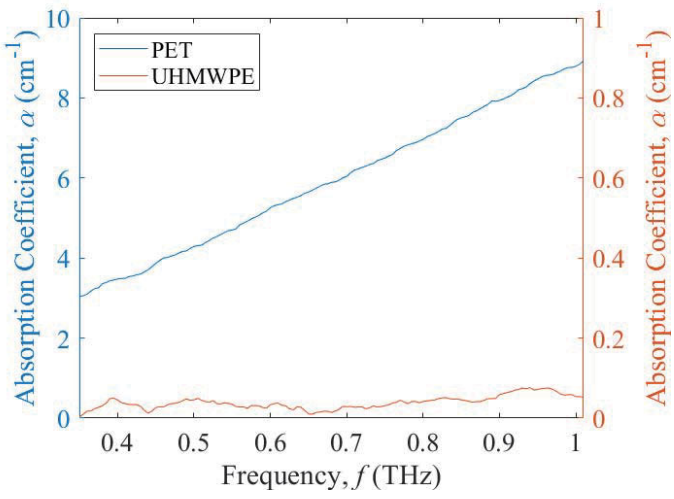

Fig. 4 The THz absorption spectrum of the 0.65-mm-thick PET sample (blue curve) and 25.6-mm-thick UHMWPE sample (red curve). The figure shows increasing PET absorption coefficient with increasing frequency up to 8.9 cm^{-1} at 1.0 THz. In contrast, UHMWPE shows a low absorption coefficient, being below 0.2 cm^{-1}.

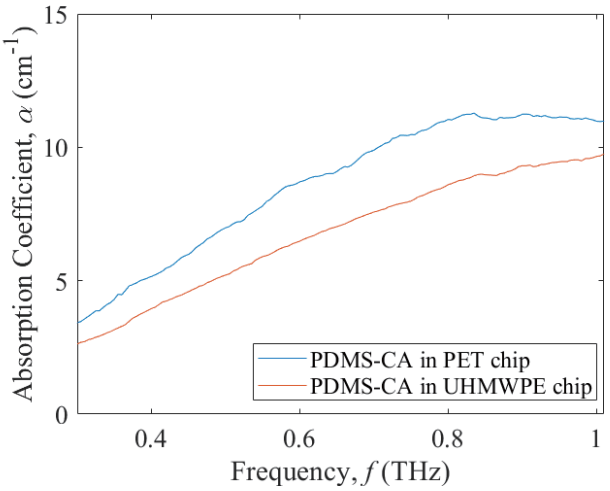

Fig. 6 The THz absorption spectrum of PDMS-CA in the PET chip (blue curve) and UHMWPE chip (red curve), formed with two layers of PET (or UHMWPE) in a 76-µm-thick THz chip window. A platform of PMMA is used with a hole diameter of 50.8 mm.

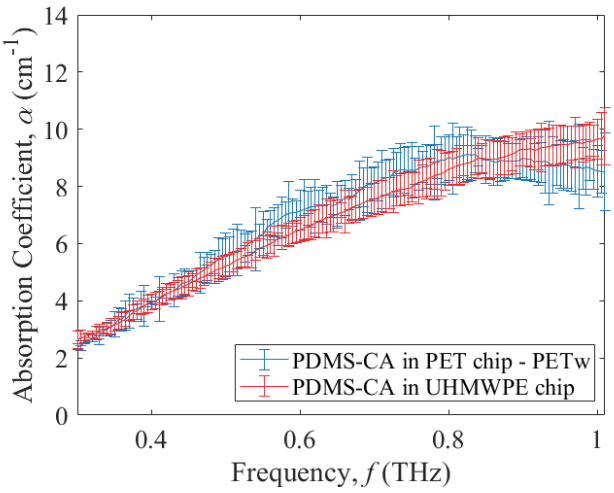

Fig. 7 The THz absorption spectrum of PDMS-CA in the PET chip after removing the PET windows absorption (blue curve) and in the UHMWPE chip without removing the UHMWPE windows absorption (red curve). The results are shown in the range from 0.35 to 1.0 THz with error bars defined according to measurement error.

Figure 7 shows the THz absorption coefficient of PDMS-CA as a function of frequency, *f*, including the predicted measurement error in the PET chip after removing the window absorption (blue curve) and in the UHMWPE chip (red curve). We see that the two spectra match each other in some points below 0.8 THz. However, the fluid absorption in PET shows disparities after this frequency. The error varies based upon the chip material and frequency. The measurement error is based upon three different measurements of each chip, and the error is defined with respect to the average absorption spectra. In the frequency range from 0.35 to 1.0 THz, the PDMS-CA absorption in the UHMWPE chip shows variation lower than the PET chip. This can be explained by the higher THz signal through the UHMWPE in comparison to PET, as shown in Fig. 3. Due to the slight decay of the THz signal after 0.8 THz, the SNR decreases in both chips, which leads to increased measurement error in Fig. 7. Furthermore, as the PET polymer shows high absorption at the higher frequencies, as shown in Fig. 4, its THz signal decays faster than UHMWPE, which has decreased SNR and appears with large error in the frequencies of 0.8 to 1.0 THz. This can explain the uncertainty in this range that appears in Fig. 6. The highest absorption value appears at 0.83 THz for the PDMS-CA in the PET chip after removing the PET window's absorption. This maximum absorption coefficient is a result of the dynamic range of the measured amplitude, the refractive index of the material, and the thickness [13]. The absorption coefficient of the PET chip is limited by its maximum measurable absorption coefficient after 0.83 THz, which appears in the absorption spectrum as a decay after 0.83 THz. In contrast, the absorption spectrum of PDMS-CA in the UHMWPE chip has an increasing trend in the scanned range with no limitation due to the maximum measurable absorption. The PDMS-CA in the UHMWPE chip shows minimal measurement error with no influence of the maximum measurable absorption in the targeted range.

IV. Conclusion

This work investigated the integration a microfluidic chip and THz spectroscopy while considering the fabrication cost and THz detection accuracy of the materials. The micro-fabricated chips that were designed, fabricated, and tested were based upon two low-cost polymers: PET and UHMWPE. The absorption coefficient of the two polymers were compared. It was found that UHMWPE has a near-zero THz absorption coefficient in the range of 0.35 to 1.0 THz. As a proof-of-concept test, chips were fabricated using the two polymers and PDMS-CA was tested as a representative low-absorption fluid. The results showed greater accuracy in measuring the absorption coefficient of PDMS-CA for the chip fabricated with UHMWPE, in comparison to the chip fabricated with PET. Moreover, a higher uncertainty was observed for the PET chip in the range of 0.8 to 1.0 THz, due to the high absorption coefficient of the polymer in this range and the resulting maximum measurable absorption. Ultimately, it was found that UHMWPE can be a low-cost and high-performance material for future microfluidic-based THz-TDS systems.

References

[1] G. R. Jha. *Terahertz Sources and Antennas for Next Generation Communication*. Switzerland: Springer International Publishing, 2014.
[2] P. H. Siegel, "Terahertz Technology," *IEEE Transactions on Microwave Theory and Techniques*, vol. 50, pp. 910-928, 2002.
[3] P. R. Smith, D. H. Auston, and M.C. Nuss, "Subpicosecond Photoconducting Dipole Antennas," *IEEE Journal of Quantum Electronics,* vol. 24, pp. 255-260, 1988.
[4] S. D. e. al, "The 2017 terahertz science and technology roadmap," *Journal of Physics D: Applied Physics*, vol. 50, pp. 12-14 2017.
[5] S. Nishizawa, K. Sakai, M. Hangyo, T. Nagashima, M. Wada Takeda, K. Tominaga, A. Oka, K. Tanaka, and O. Morikawa. "*Terahertz Time-Domain Spectroscopy*" in *Terahertz Optoelectronics*, Springer, Berlin, Heidelberg, 2005, pp. 203-270.
[6] Q. Tang, M. Liang, Y. Lu, P. K. Wong, G. J. Wilmink, D. D. Zhang, and H. Xin, "Microfluidic Devices for Terahertz Spectroscopy of Live Cells Toward Lab-on-a-Chip Applications," *Sensors (Basel, Switzerland*), vol. 16, 476 pp 1-11, 2016.
[7] J. C. McDonald, D. C. Duffy, J. R. Anderson, D. T. Chiu, H. Wu, O. J. Schueller, and G, M. Whitesides, "Fabrication of microfluidic systems in poly(dimethylsiloxane)," *Electrophoresis*, vol. 21, pp. 27-40, 2000.
[8] M. Leester-Schädel, T. Lorenz, F. Jürgens, and C. Richter. *Fabrication of Microfluidic Devices*. Switzerland, Springer, Cham, 2016.
[9] J. C. McDonald and G. M. Whitesides, "Poly(dimethylsiloxane) as a material for fabricating microfluidic devices," *Accounts of Chemical Research,* vol. 35, pp. 491-499, 2002.
[10] A. Podzorov and G. Gallot, "Density of states and vibrational modes of PDMS studied by terahertztime-domain spectroscopy," *Chemical Physics Letters,* vol. 495, pp. 46-49, 2010.
[11] A. Podzorov and G. Gallot, "Low-loss polymers for terahertz applications," *Applied Optics*, vol. 37, pp. 3254-3257, 2008.
[12] W. Withayachumnankul, B. M. Fischer, and D. Abbott, "Material thickness optimization for transmission-mode terahertz time-domain spectroscopy," *Optics Express*, vol. 16, pp. 7382-7396, 2008.
[13] P. U. Jepsen and B. M. Fischer, "Dynamic range in terahertz time-domain transmission and reflection spectroscopy," *Optics Letters 29,* vol. 30, pp. 29-31, 2005.